New Effective-Nuclei Concept for Simplified Analysis of Batch Crystallization

Masaaki Yokota, Akira Sato, and Noriaki Kubota
Dept. of Applied Chemstry and Molecular Science, Iwate University, 4-3-5 Ueda, Morioka 020, Japan

A new ''effective nuclei'' concept for a simplified approach to the analysis of batch crystallization with agglomeration is proposed. The new effective-nuclei concept comes from agglomeration characteristics observed experimentally in a batch crystallizer. Small-sized crystals could combine with both large-sized crystals and each other. Agglomeration among large-sized crystals can be neglected. From these experimental results, new effective nuclei are defined as crystals at a size-boundary between small-sized crystals and large-sized crystals. By taking into account only large-sized crystals in formulating population balance equation, the agglomeration term can be omitted. The analytical solution of the population balance equation is induced for an ideal batch-cooling case (constant supersaturation and constant effective growth rate of crystal). The solution explains measured data well.

Introduction

Analysis of the crystal size distribution (CSD) in a crystallizer provides us much valuable information, such as crystal growth and nucleation rates, which are required for the design of optimal operation of an industrial crystallizer. For CSD analysis, a commonly used technique in the field of industrial crystallization is to formulate a population balance equation and then solve it. A typical example that has been successfully applied for industrial purposes is the model of Randolph and Larson (1988). They showed that CSD obtained from a continuous mixed-suspension, mixed-product-removal (CMSMPR) crystallizer at a steady state can be described by Eq. 1:

$$u(L) = u_0 \exp\left(-\frac{L}{G\cdot\tau}\right). \tag{1}$$

As can be seen in Eq. 1, the semilogarithmic plot of population density, $u(L)$, vs. crystal size, L, yields a straight line; and the growth rate of crystals, G, and quantity of (true) nuclei, u_0, can be estimated from the slope and intercept of the straight line at a given residence time, τ. Additionally, the nucleation rate, B, can be estimated as $B = G\cdot u_0$. This is a very simple and elegant method, and this simpilicity has made Randolph and Larson's model a widely used method for analyzing CSD.

In most actual crystallizers, however, agglomeration, which is not taken into account in Randolph and Larson's model, does occur together with nucleation and growth (agglomerating system). In an agglomerating system, we must formulate a complicated population balance equation (Hounslow et al., 1988; Hounslow, 1990a,b) as

$$\frac{d[G(L)\cdot u(L)]}{dL} + \frac{u(L)}{\tau} = \frac{L^2}{2}\int_0^{L_k} \frac{\left[(L^3-\lambda^3)^{1/3},\lambda\right] u\left[(L^3-\lambda^3)^{1/3}\right] u(\lambda)\, d\lambda}{(L^3-\lambda^3)^{2/3}} - u(L)\int_0^{\infty} k(L,\lambda)u(\lambda)\, d\lambda, \tag{2}$$

Correspondence concerning this article should be addressed to M. Yokota.

for a continuous system, and

$$\frac{\partial u(L,t)}{\partial t} + \frac{\partial [G(L,t)\cdot u(L,t)]}{\partial L} = \frac{L^2}{2}\int_0^{L_k} \frac{\beta\left[(L^3-\lambda^3)^{1/3},\lambda\right] u\left[(L^3-\lambda^3)^{1/3}\right] u(\lambda,t)\, d\lambda}{(L^3-\lambda^3)^{2/3}} - u(L,t)\int_0^{\infty} k(L,\lambda)u(\lambda,t)\, d\lambda, \quad (3)$$

for a batch system. The first term on the righthand side of Eqs. 2 and 3 is the birth rate of crystals caused by agglomeration and the second term is the death rate caused by agglomeration. Function $k(L,\lambda)$ in Eqs. 2 and 3 is called the agglomeration kernel. Recently, many researchers have developed calculation algorithms to solve the preceding integrodifferential equations numerically (Bramley et al., 1997; David et al., 1995; Glatz et al., 1986; Halfon and Kaliaguine, 1976; Hounslow et al., 1988; Hounslow, 1990a,b; Lamey et al., 1986; Lui and Thompson, 1992; Marchal et al., 1988; Mumtaz et al., 1997; van Peborgh Gooch et al., 1996; Wojcik and Jones, 1997; Yokota and Kubota, 1996; Zukoski et al., 1996). Owing to their efforts, numerical solutions can be obtained in some agglomerating systems (traditional approach), and the time required for calculation has become shorter due to the rapid progress in computer technology. We consider the traditional approach to be useful only for simulation purposes, but it is difficult to apply it to analysis of an observed CSD. There are also other technical problems in the traditional approach, such as the agglomeration kernel. Although some mathematical models for the agglomeration kernel have been proposed, it is very difficult to experimentally prove the validity of a proposed model. It is agglomeration that causes complicated problems in solving a population-balance equation. Thus, if we can omit the agglomeration term in a population-balance equation even in an agglomerating system, a simpler method can be obtained.

Here, we want to point out what will happen if we change the widely accepted nuclei concept. Nuclei are considered to have an almost zero size (nanolevel), which can be approximated to zero compared with the size of the product crystals (some tens of micrometers to a few millimeters). In formulating a population balance equation, the whole size range of crystals (zero to infinity) existing in a crystallizer is often taken into account. As long as a zero-to-infinity size range is considered in formulating a population balance equation for an agglomerating system, we cannot avoid the integrodifferential equation, because agglomeration must occur somewhere in the size range of zero to infinity. Here, the question arises as to why we have to take into account the whole size range in analyzing CSDs of the product from an actual crystallizer.

In this study, we found experimentally some interesting agglomeration characteristics in batch system. Small-sized crystals could combine both with large-sized crystals and with each other. Agglomeration among large-sized crystals can be neglected. Based on these experimental results, we defined new ''effective nuclei'' as particles at the size boundary of small-sized crystals and large-sized crystals. The effective nuclei concept successfully omits the agglomeration term in formulating a population-balance equation, and analytical solution is easily obtained. We show typical experimental data (potash-alum) that can be elegantly analyzed using the analytical solution.

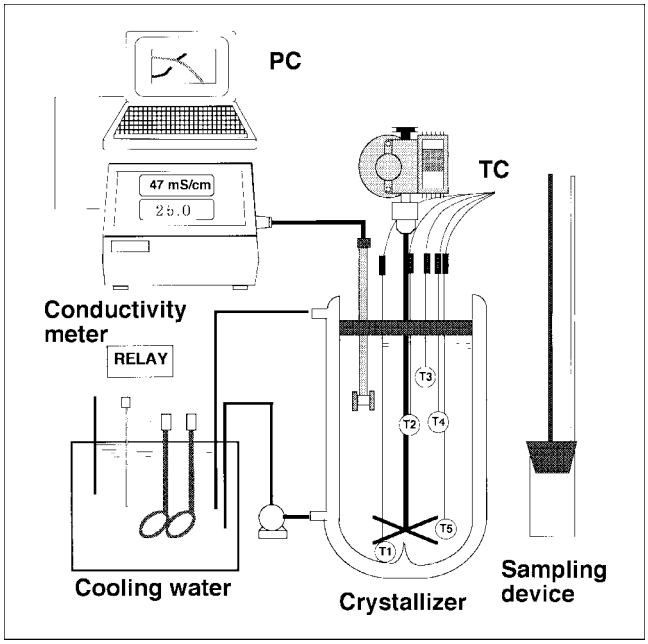

Figure 1. Experimental setup for batch-cooling crystallization of potash alum.

Experimental Studies

The experimental apparatus is shown in Figure 1. It is composed of a 6-L capacity jacketed glass crystallizer, a cooling water bath (283 K), an electrical conductivity measurement instrument (digital conduct meter CM-40 fitted with an electrode cell CG511A, TOA Electronics Ltd., Japan), and a thermometer. This apparatus enables on-line measurement of the solution concentration and supersaturation during batch-cooling crystallization (Hlozny et al., 1992; Jagadesh et al., 1996).

Using the apparatus just described, a typical batch run was performed as follows. An aqueous solution of potash alum saturated at 313 K was prepared directly in the crystallizer. The solution was maintained at 318 K (undersaturated) for 60 min to make the solution crystal-free, and then it was cooled slowly. When the desired level of supersaturation was achieved, a known amount of seed crystals, rinsed with distilled water, were introduced into the crystallizer to start crystallization. A new formation of an excess amount of small crystals must be avoided during batch crystallization in order to produce large- and uniform-sized crystals. This is a common target in batch crystallization. In order to meet this demand, it is widely recommended that the supersaturation be kept nearly constant within the metastable zone (Mullin, 1993; Gutwald and Mersmann, 1990). Therefore, we controlled the cooling profile manually so as to maintain a constant (lower) level of supersaturation, ΔC, during the batch run. However, since we did not know a suitable supersaturation level, we

carried out several runs at different constant supersaturation levels. During the batch run, concentration and temperature of the solution were automatically recorded at 60-s intervals. We also measured transient size distributions of the suspended crystals at about 60-min intervals. Sampling of suspension was carried out using the device shown in Figure 1, which is simply an acrylic resin cylindrical cup (40 cm^3) fitted with a rubber cap. On sampling, we inserted the sampling cup into the suspension and quickly lifted the rubber cap to introduce the suspension into the cup, and then we covererd it again and took it out of the suspension. About 10 s were needed for one sampling. The size distribution of crystals was measured by sieving (lowest measurable size = 100 μm). We sometimes measured the size distribution of crystals less than 100 μm through an optical microscope. When prescribed amounts of crystals (W_p) were obtained, we finished the run. The impeller speed was maintained at 300 min^{-1} to keep the crystals suspended as homogeneously as possible.

The amount of seed crystals introduced, W_s, was decided as follows. Assuming an ideal batch operation (negligible formation of nuclei during the batch), a simple equation can be formulated by mass balance:

$$W_s = W_p \times \left(L_s/L_p \right)^3, \tag{4}$$

where L and W are the average size and weight of crystals, respectively; and subscripts s and p mean seed crystals and product crystals, respectively. Using Eq. 4, the amount of seed crystals, W_s, can be decided by giving the desired value of L_p, W_p, and initial condition of L_s. In our case, W_p = 540 g, L_p = 1,000 μm, and L_s = 400 μm; then W_s = 34.56 g. The size distribution of seed crystals introduced can be seen in Figure 2.

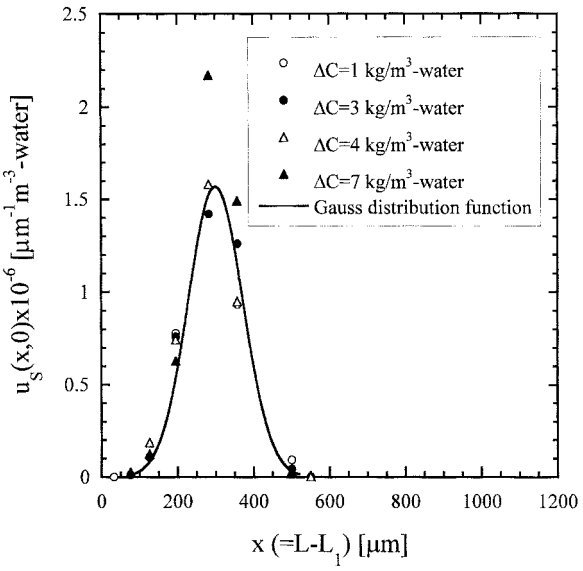

Figure 2. Initial size distribution of seed crystals introduced in the batch-crystallization experiment.

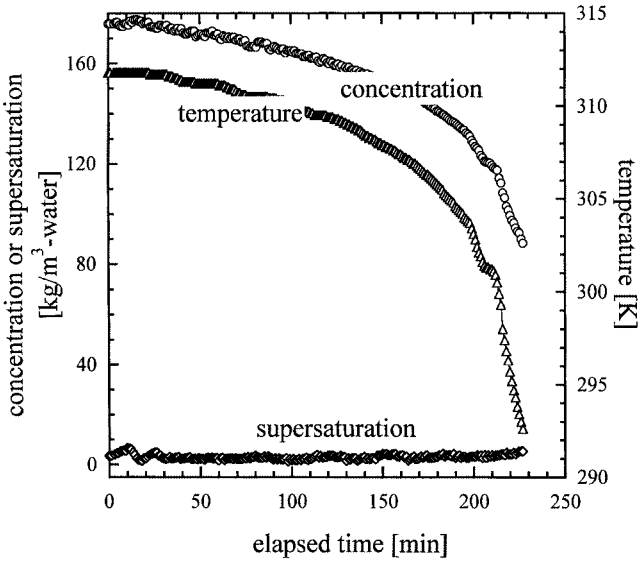

Figure 3. Example of transient supersaturation, concentration and temperature during batch crystallization of potash alum.

ΔC = 3 kg−hydrate/m^3−water, impeller speed = 300 min^{-1}.

Results and Discussion

Experimental results

Figure 3 shows the transient solution concentration and temperature data measured in a typical batch run (supersaturation, ΔC = 3 kg−hydrate/m^3−water). As can be seen in this figure, the solution concentration (○) decreases very slowly in the early stage of the run. Growth of the seed crystals introduced was the dominant phenomenon in this stage. Nucleation commenced in the middle stage of the run, and then the concentration began to decrease rapidly due to the growth of the nuclei. In compensation for this rapid decrease in the concentration, we had to cool the solution rapidly (Δ) in order to maintain the supersaturation (◇) at a given constant level. As can be expected from this concentration curve, the suspension density of the crystals (M_T) increased exponentially, as shown in Figure 4 (data obtained from typical three runs are drawn). Lines in the figure were drawn empirically using an exponential function as

$$M_T(t) = p \exp(q \cdot t). \tag{5}$$

Here, p, q are adjusting parameters. Equation 5 is utilized in a later section.

Figures 5a and b show two typical transient cumulative oversize distributions measured using an optical microscope. At ΔC = 3 kg−hydrate/m^3−water (Figure 5a), transient CSDs were observed, to show the apparent simultaneous occurrence of growth and nucleation. At ΔC = 7 kg−hydrate/m^3−water, the increase in the number of crystals continued until t = 40 min (Figure 5b). After that, however, it began to decrease, and the size distribution curves cross at about L = 100 μm. This means that the crystals smaller than 100-μm

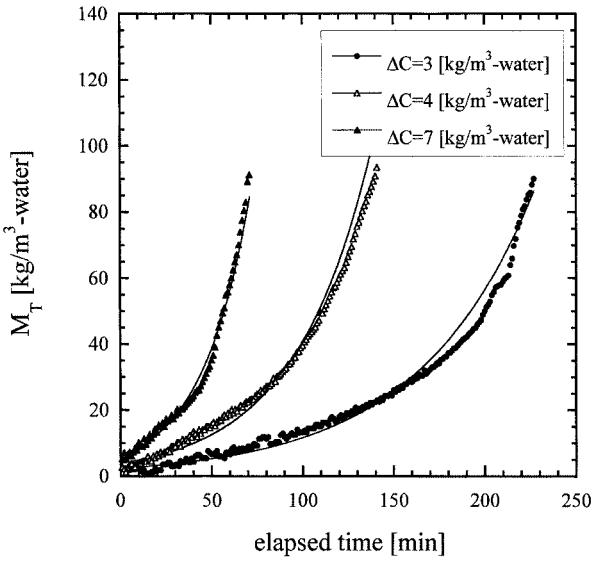

Figure 4. Typical example of transient suspension density of crystals, M_T, during batch crystallization of potash alum.

agglomerate with each other and/or with other crystals larger than 100 μm. Microscopic observation of crystals sampled between 40 and 60 min at $\Delta C = 7$ kg−hydrate/m^3−water supports this speculation. Here we note that the occurrence of agglomeration was found not only in this period but also during the other period (Figure 5b) and/or in other runs. In any case, however, agglomeration between crystals larger than 100 μm was seldom found. The reason why agglomeration occurred frequently enough to decrease the total number of crystals only when $40 < t < 60$ min ($\Delta C = 7$ kg−hydrate/m^3−water) is not known. Anyway, agglomeration must be taken into account in modeling crystallization. The key point is how to deal with agglomeration. Fortunately, we were able to estimate the agglomeration characteristics of the potash alum−water system, as mentioned earlier, which made it much easier for us to describe the crystallization behavior (see the next section).

Simplified model for analysis of batch crystallization using the new effective-nuclei concept

Before discussing the model, we explain the reasons why a new effective-nuclei concept is needed. There are two reasons: (1) any CSD measurement method (sieve analysis, electrical zone-sensing method, optical method, photographic method, etc.) has a lower limit of detection, which generally ranges from a few micrometers to 100 μm. In our case (sieve analysis), the lowest measurable size was 100 μm. No instruments can detect true nuclei (nanolevel), especially in industrial crystallizers using such detectors. The number of nuclei is often determined by extrapolation as in Randolph and Larson's model for CMSMPR. However, is there any known reason why we must know the formation rate of nearly zero-sized particles? Formation of zero-sized particles must occur in a complicated way. There must be many sources of formation of zero-sized particles (primary and secondary nucleations). There is no single equation to describe the rate of formation of these particles. Further, we must ask, what is there of merit in knowing such a "true" nucleation rate? What is needed is a more convenient and practical nuclei concept that makes it much easier to analyze the actual crystal size distribution. (2) The other reason is related to mathematical problems. As mentioned earlier, small-sized crystals of nondetectable size can combine with both large-sized crystals and with each other. However, collisions between large-sized crystals are not effective for forming agglomerates. Thus, if we consider the population balance by ignoring crystals of nondetectable size, the agglomeration term in the balance equation is automatically dropped.

Based on the preceding background, we distinguish potash−alum crystals existing in the crystallizer according to their size as follows (see also Figure 6). Crystals that are smaller than the smallest measurable size ($L_1 = 100$ μm in this study) are defined as "subnuclei." "Effective nuclei" are

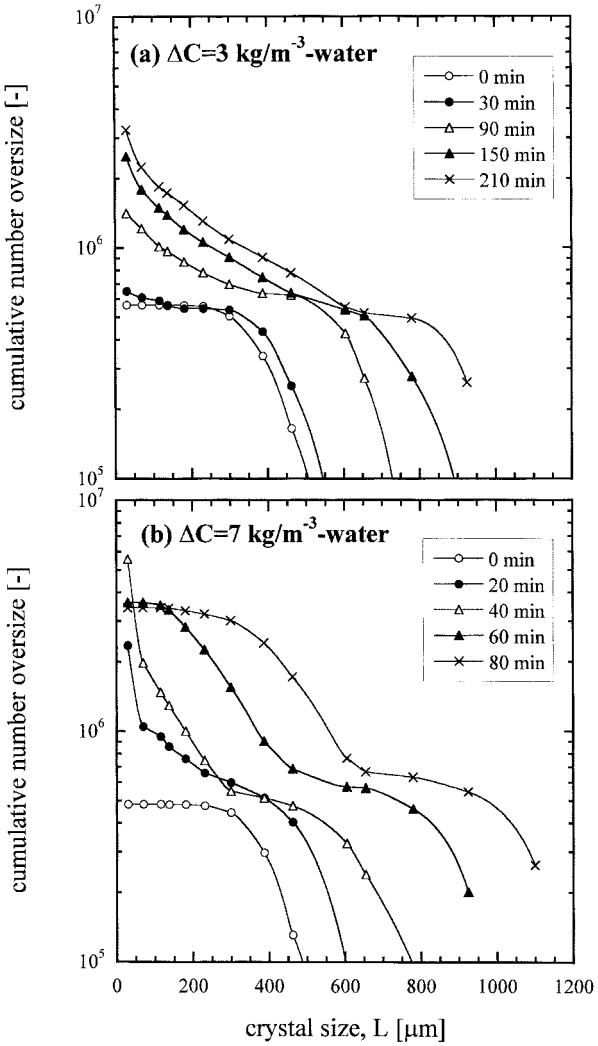

Figure 5. Transient cumulative number oversize distribution of potash alum crystals during the batch crystallization.

(a) $\Delta C = 3$ kg−hydrate/m^3−water, impeller speed = 300 min^{-1}; (b) $\Delta C = 7$ kg−hydrate/m^3−water, impeller speed = 300 min^{-1}.

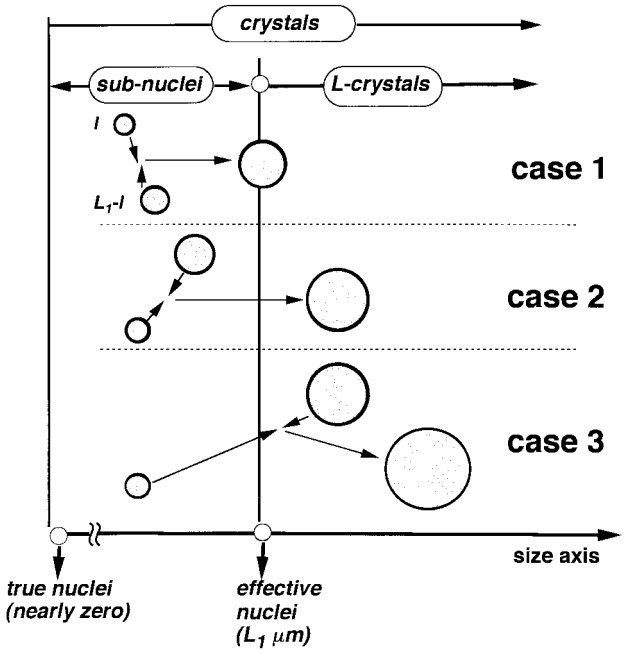

Figure 6. Definition of L-crystals, subnuclei, and effective nuclei for simplification of analysis of the crystallization processes.

the crystals of size L_1. Additionally, we define crystals larger than L_1 as "L-crystals." It should be noted here that the definition of our effective nuclei is much different from the widely accepted one.

Now, we can describe the model mathematically by incorporating the following simplifying assumptions.

1. *Effective nucleation rate:* Two possible mechanisms of the formation of new L-crystals must be considered: one is the formation of effective nuclei by growth of subnuclei, and the other is the formation of effective nuclei (case 1 in Figure 6) and/or new L-crystals caused by agglomeration among subnuclei (case 2). In such cases, the size-dependent effective nucleation rate should be drawn as can be expected from Figure 6. In this article, however, case 2 is omitted and the effective nucleation rate is defined as the formation rate of effective nuclei.

2. *Agglomeration:* Subnuclei can adhere to L-crystals (case 3 in Figure 6) and can combine with them. However, agglomeration does not occur between L-crystals.

3. *Effective growth rate:* Size enlargement due to agglomeration of subnuclei to an L-crystal (case 3 in Figure 6) is included in the growth term, as is ordinary molecular-level growth.

For mathematical simplicity, we introduce a new crystal size variable, $x\ (= L - L_1)$ instead of L, where L_1 is the smallest measurable size by sieving. By considering only crystals that are larger than effective nuclei, the general population-balance equation with agglomeration can be simplified:

$$\frac{\partial u(x,t)}{\partial t} + \frac{\partial \left[G_{\text{eff}}(x,t) \cdot u(x,t) \right]}{\partial x} = 0, \qquad x > 0,\ t > 0. \quad (6)$$

To solve this equation, both $G_{\text{eff}}(x,t)$ and $B_{\text{eff}}(t)$ must be expressed as a function of time. The two equations are considered as follows.

Effective Growth Rate. Figures 7a and b show population-density plots of L-crystals obtained for two typical runs. Let us now divide L-crystals into two groups (S-crystals and N-crystals) according to their age. L-crystals appearing at $t = 0$ (seed crystals) are called as S-crystals, while the ones newly formed after $t = 0$ are called N-crystals. In Figures 7a and 7b, the size distribution of the S-crystals (S-CSD) moves to the right in parallel at an almost constant rate. This means that the effective growth rate of S-crystals is (apparently) sizeindependent during a batch run. So, the effective growth rate of L-crystals (S- +N-crystals) may be (at least in our case) size- and time-dependent:

$$G_{\text{eff}}(x,t) = G_{\text{eff}}. \quad (7)$$

Effective Nucleation Rate. The effective nucleation-rate equation is assumed to be analogous to the usual nucleation-

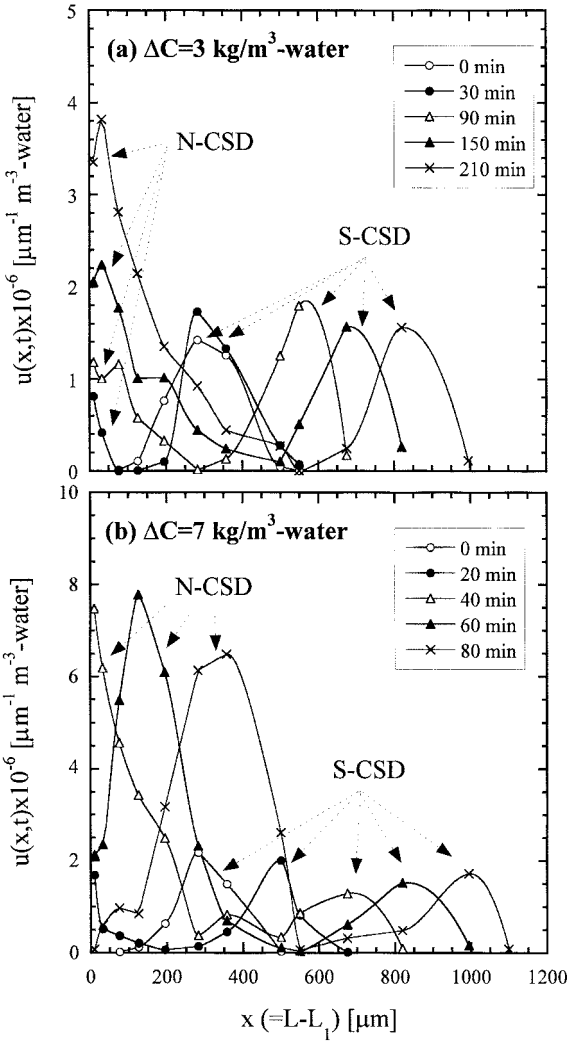

Figure 7. Transient size distribution of L-crystals of potash alum during the batch crystallization.

(a) $\Delta C = 3$ kg-hydrate/m^3-water, impeller speed = 300 min^{-1}; (b) $\Delta C = 7$ kg-hydrate/m^3-water, impeller speed = 300 min^{-1}.

rate equation:

$$B_{\text{eff}}(t) = k_b \cdot G_{\text{eff}}^{i} M_T^{b}(t) = K_B \cdot M_T^{b}(t). \quad (8)$$

Here, $K_B = k_b \cdot G_{\text{eff}}^{i}$.

Now, Eq. 6 can be rewritten as

$$\frac{\partial u(x,t)}{\partial t} + G_{\text{eff}} \frac{\partial u(x,t)}{\partial x} = 0, \qquad x > 0, \quad t > 0 \quad (9)$$

$$B.C.: u(x,0) = \Psi(x), \quad (10)$$

$$B.C.: u(0,t) = B_{\text{eff}}(t)/G_{\text{eff}}, \quad (11)$$

where $\Psi(x)$ is the size distribution function of the seed crystals that were introduced initially. A general solution of these equations can be easily obtained by the method of characteristics.

For S-crystals (seed crystals, $x > G_{\text{eff}} \cdot t$),

$$u_S(x,t) = \Psi(x - G_{\text{eff}} \cdot t). \quad (12)$$

We prepared seed crystals having a Gauss distribution (Figure 2). Then, $\Psi(x)$ can be given as

$$\Psi(x) = \alpha \cdot \exp\left[-\frac{(x-\mu)^2}{\beta}\right]. \quad (13)$$

Finally, S-CSD becomes

$$u_S(x,t) = \alpha \cdot \exp\left[-\frac{(x - G_{\text{eff}} \cdot t - \mu)^2}{\beta}\right]. \quad (14)$$

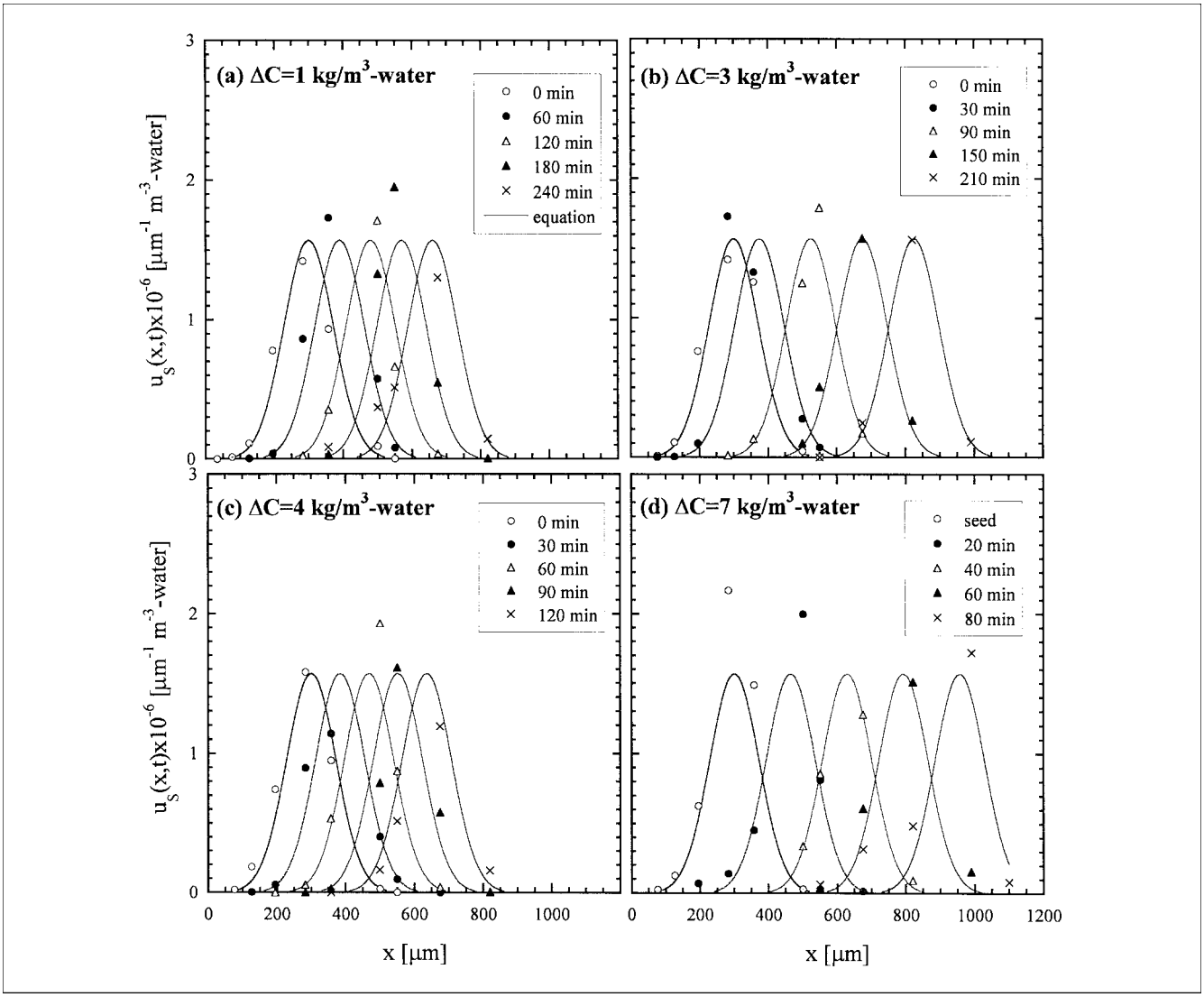

Figure 8. Comparison of measured population density of S-crystals vs. size plot with equation (ref) (lines).

(a) $\Delta C = 1$ kg−hydrate/m^3−water; (b) $\Delta C = 3$ kg−hydrate/m^3−water; (c) $\Delta C = 4$ kg−hydrate/m^3−water; (d) $\Delta C =$ kg−hydrate/m^3−water; impeller speed = 300 min^{-1}.

On the other hand, the size distribution of N-crystals ($x < G_{\text{eff}} \cdot t$) can be given as

$$u_N(x, t) = B_{\text{eff}}(t - x/G_{\text{eff}})/G_{\text{eff}} = \frac{K_B}{G_{\text{eff}}} \cdot M_T^b(t - x/G_{\text{eff}}). \quad (15)$$

Since suspension density of crystals (M_T) is experimentally given as in Eq. 5, N-CSD can be expressed as

$$u_N(x, t) = \frac{K_B}{G_{\text{eff}}} \cdot \{ p \cdot \exp[q \cdot (t - x/G_{\text{eff}})] \}^b = \gamma \cdot \{ \exp[q \cdot (t - x/G_{\text{eff}})] \}^b, \quad (16)$$

where $\gamma = (K_B/G_{\text{eff}})p^b$.

In the case of batch crystallization with agglomeration, it is usually very difficult to obtain an analytical solution of the population-balance equation (Eq. 3). However, the effective-nuclei concept proposed in this study makes the analytical solution (Eqs. 14 and 16) possible with the help of some simplified assumptions. Comparison of the obtained solutions with measured CSDs (S-CSD and N-CSD) is described in the next section.

Comparison of measured CSDs with Equations 14 and 16

S-CSDs. Comparison results are shown in Figures 8a–d. Plots are the measured data, while the lines are fitted curves using Eq. 14. In all cases, it can be understood that Eq. 14 successfully explains the measured data.

The estimated effective growth rate G_{eff} is plotted against supersaturation in Figure 9. An interesting result was seen in the figure. The effective growth rate at $\Delta C = 7$ kg–hydrate/m^3–water was much higher than the value obtained by extrapolating from the values at lower ΔC. Our G_{eff} includes size-enlargement caused by agglomeration between subnuclei and L-crystals in addition to ordinary molecular-level growth. The extremely high growth rate at high supersaturations may be due to the occurrence of frequent agglomeration between subnuclei and L-crystals.

If one introduces seed crystals that have exponential size distribution:

$$\Psi(x) = \eta \exp(-\nu \cdot x), \quad (17)$$

more elegant analysis of measured S-CSD is possible. In this case, S-CSD can be drawn as

$$u_S(x, t) = \eta \exp[-\nu \cdot (x - G_{\text{eff}} \cdot t)]. \quad (18)$$

Taking the logarithm of Eq. 18, one gets

$$\ln u_S(x, t) = \ln \eta + \nu \cdot G_{\text{eff}} \cdot t - \nu \cdot x. \quad (19)$$

Since S-CSD at $t = 0$ [$u_S(x, 0)$] is given initially, two parameters (η and ν) in Eq. 19 can be estimated by simply using

$$\ln u_S(x, 0) = \ln \eta - \nu \cdot x. \quad (20)$$

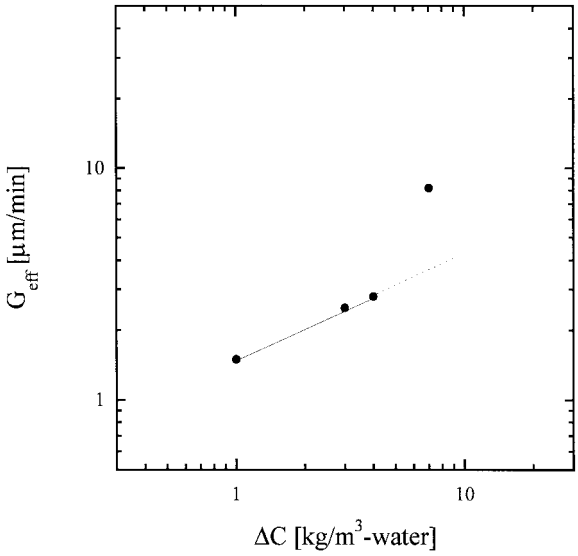

Figure 9. Correlation between effective growth rate, *G*′, of potash alum crystals and supersaturation (impeller speed = 300 min^{-1}).

So the semilogarithmic plot of measured $u_S(x, t)$ vs. size, x, gives a straight line. Reading the intercept of a straight line (at $x = 0$), the effective growth rate can be estimated as

$$G_{\text{eff}} = \frac{\text{Intercept} - \ln \eta}{\nu \cdot t}. \quad (21)$$

N-CSDs. In comparing measured N-CSD with Eq. 16, it is convenient to use a logarithmic form of Eq. 16:

$$\ln u_N(x, t) = \ln \gamma + b \cdot q \cdot (t - x/G_{\text{eff}}). \quad (22)$$

Since G_{eff} was given previously by analyzing S-CSDs, we can plot measured $u_N(x, t)$ against $(t - x/G_{\text{eff}})$. If Eq. 22 is applicable, a straight line will be given. Comparison results are shown in Figures 10a–d. Except for Figure 10d, straight lines are successfully obtained. As can be understood from Eq. 22, the slope of a straight line gives $b \cdot q$. In our case, q is given by fitting Eq. 5 with measured M_T for each run (Figure 4). So, one of the two kinetic nucleation parameters b can be estimated by dividing the slope by q. As a result, $b = 1$ is calculated independently of supersaturation. This is a reasonable result. Now, if we know G_{eff}, p, and b, then another effective nucleation parameter K_B can be estimated with a relation $\gamma = (K_B/G_{\text{eff}})p^b$ described in the previous section. In our case, $K_B = 5.7 \times 10^5$ (independent of supersaturation).

When $t = 60$ and 80 min at $\Delta C = 7$ kg–hydrate/m^3–water, $\ln u_N(x,t)$ vs. $t - G_{\text{eff}}$ plots have maxima (Figure 10d). This result is very interesting and must be closely related to the sudden change in the frequency of agglomeration (between subnuclei and/or agglomeration of subnuclei to large-sized crystals). As mentioned in Figure 5b, the frequency of the agglomeration rapidly increased midway in the run, leading to loss of subnuclei. As a result, effective nucleation stopped suddenly after that time. On the other hand, we employed the same kind of equation with the ordinal nucleation-rate

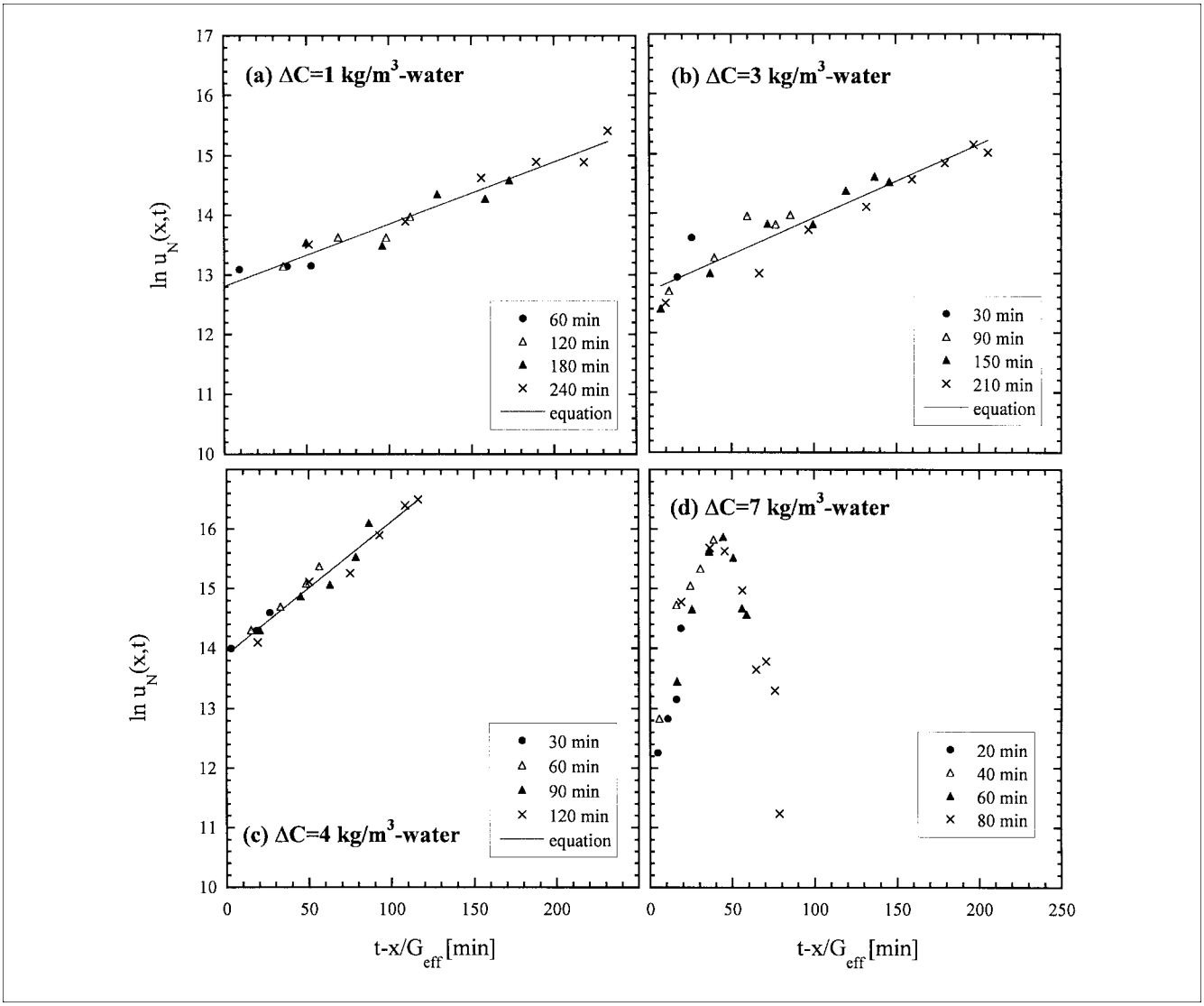

Figure 10. Comparison of measured population density of S-crystals vs. size plot with equation (ref) (lines).

(a) $\Delta C = 1$ kg–hydrate/m^3–water; (b) $\Delta C = 3$ kg–hydrate/m^3–water; (c) $\Delta C = 4$ kg–hydrate/m^3–water; (d) $\Delta C = 7$ kg–hydrate/m^3–water; impeller speed = 300 min^{-1}.

equation (power function, Eq. 8). In the power function, such a factor as the reduction in (apparent) nucleation rate is not included. Therefore, the new nucleation rate is needed to explain the N-CSDs in Figure 10d, because N-CSD is closely related to the effective nucleation rate, as can be understood from Eq. 15. Further investigation of the new nucleation rate is needed.

Determination of the effective nuclei size, L_1

We can now conclude that our new effective-nuclei concept gives us an analytical solution for CSD in batch crystallization with agglomeration. As mentioned previously, our model assumes that small-sized particles (subnuclei) can combine with both large-sized particles (L-crystals) and with each other. Agglomeration among L-crystals can be neglected. We believe that this agglomeration characteristic also exists in other systems and that our model can therefore be applied to other systems. One important problem is how to decide the size of effective nuclei (L_1). It can be easily seen that the effective nucleation rate B' changes with L_1 even in the system concerned. Therefore, we recommend taking L_1 at first as the smallest detectable size of the CSD analyzer. Then crystals should be observed microscopically. If crystals larger than L_1 agglomerate among themselves, L_1 must be redetermined so that crystals larger than L_1 do not agglomerate among themselves. Of course, our model cannot be applied if the redetermined L_1 are too large to draw the CSD curve.

Conclusions

1. Experimentally, we showed the characteristics of the agglomeration that occurred during batch crystallization (potash–alum). Smaller-sized crystals (subnuclei) can combine with both large crystals (L-crystals) and among them-

selves. Agglomeration among L-crystals can be neglected. Based on these experimental findings, we defined the new effective nuclei as the size boundary of subnuclei and L-crystals.

2. By taking only L-crystals into account in formulating population-balance equations, we can omit the agglomeration term, because agglomeration does not occur between L-crystals. We obtained analytical solutions of the population-balance equations for the batch system, as shown in Eqs. 14 and 16. The solutions explain the measured data well.

Notation

$B_{\text{eff}}(t)$ = effective nucleation rate, $\text{m}^{-3} \cdot \text{min}^{-1}$
b = power number, Eq. 8
$G(L)$, $G(L,t)$ = crystal growth rate, $\mu\text{m} \cdot \text{min}^{-1}$
$G_{\text{eff}}(L,t)$, G_{eff} = effective growth rate of crystals, $\mu\text{m} \cdot \text{min}^{-1}$
i = power number, Eq. 8
$k(L, \lambda)$ = agglomeration kernel
k_b = effective nucleation-rate coefficient, Eq. 8
t = time, min
$u(L,t)$, $u(x,t)$ = population density distribution function, $\mu\text{m}^{-1} \cdot \text{m}^{-3}$
α = parameter, Eq. 13
β = parameter, Eq. 13
η = parameter, Eq. 17
λ = size parameter, Eqs. 2 and 3
μ = parameter, Eq. 13
ν = parameter, Eq. 17

Subscript

N = newly formed crystals

Literature Cited

Bramley, A. S., M. J. Hounslow, R. Newman, W. R. Paterson, and C. Pogessi, ''The Role of Solution Composition on Agglomeration during Precipitation,'' *Trans. Inst. Chem. Eng.*, **75**(Part A), 119 (1997).

David, R., P. Marchal, and B. Marcant, ''Modeling of Agglomeration Industrial Crystallization from Solution,'' *Chem. Eng. Technol.*, **18**, 302 (1995).

Glatz, C. E., M. Hoare, and J. Landa-Vertiz, ''The Formation and Growth of Protein Precipitates in a Continuous Stirred-Tank Reactor,'' *AIChE J.*, **32**, 1196 (1986).

Gutwald, T., and A. Mersmann, ''Batch Cooling Crystallization at Constant Supersaturation,'' *Chem. Eng. Technol.*, **13**, 229 (1990).

Halfon, A., and S. Kaliaguine, ''Alumina Trihydrate Crystallization,'' *Can J. Chem. Eng.*, **54**, 160 (1976).

Hlozny, L., A. Sato, and N. Kubota, ''On-Line Measurement of Supersaturation During Batch Cooling Crystallization of Ammonium Alum,'' *J. Chem. Eng. Jap.*, **25**(5), 604 (1992).

Hounslow, M. J., R. L. Ryall, and V. R. Marshall, ''A Discretized Population Balance for Nucleation, Growth, and Aggregation,'' *AIChE J.*, **34**(11), 1821 (1988).

Hounslow, M. J., ''A Discretized Population Balance for Continuous Systems at Steady State,'' *AIChE J.*, **36**(1), 106 (1990a).

Hounslow, M. J., ''Nucleation, Growth, and Agglomeration Rates from Steady-State Experimental Data,'' *AIChE J.*, **36**(11), 1748 (1990b).

Jagadesh, D., N. Kubota, M. Yokota, A Sato, and N. S. Tavare, ''Large and Monosized Product Crystals from Natural Cooling Mode Batch Crystallizer,'' *J. Chem. Eng. Jpn.*, **29**(5), 865 (1996).

Lamey, M. D., and T. A. Ring, ''The Effect of Agglomeration in a Continuous Stirred Tank Crystallizer,'' *Chem. Eng. Sci.*, **41**, 1213 (1986).

Lui, R. Y. M., and Thompson, R. W., ''Analysis of a Continuous Crystallizer with Agglomeration,'' *Chem. Eng. Sci.*, **47**, 1897 (1992).

Marchal, P., R. David, J. P. Klein, and J. Villermaux, ''Crystallization and Precipitation Engineering,'' *Chem. Eng. Sci.*, **43**, 59 (1988).

Mullin, J. W., *Crystallization*, 3rd ed., Butterworth-Heinemann, London (1993).

Mumtaz, H. S., M. J. Hounslow, N. A. Seaton, and W. R. Paterson, ''Orthokinetic Agglomeration During Precipitation,'' *Trans. Inst. Chem. Eng.*, **75**(Part A), 152 (1997).

Randolph, A. D., and M. A. Larson, *Theory of Particulate Processes*, 2nd ed., Academic Press, New York (1988).

Van Peborgh Gooch, J. R., M. J. Hounslow, and J. Mydlarz, ''Discriminating Between Size-Enlargement Mechanisms,'' *Trans. Inst. Chem. Eng.*, **74**(Part A), 803 (1996).

Wojcik, J. A., and A. G. Jones, ''Experimental Investigation into Dynamics and Stability of Continuous MSMPR Agglomerative Precipitation of $CaCO_3$ Crystals,'' *Trans. Inst. Chem. Eng.*, **75**(Part A), 113 (1997).

Yokota, M., and N. Kubota, ''Apparent Size-Dependent Growth of Potash Alum Crystals by Agglomeration,'' *AIChE J.*, **42**(4), 1170 (1996).

Zukoski, D. F., D. F. Rosenbaum, and P. C. Zamora, ''Agglomeration in Precipitation Reactions,'' *Trans. Inst. Chem. Eng.*, **74**(Part A), 723 (1996).

Manuscript received Dec. 23, 1997, and revision received Apr. 16, 1999.